Research paper

Fabrication of mesoscale topographical gradients in bulk titanium and their use in injection moulding

Andrew Connell *, Paul M. Reynolds, Anwer Saeed, Nikolaj Gadegaard *

Division of Biomedical Engineering, University of Glasgow, Glasgow G12 8LT, UK

ABSTRACT

Fabrication methods for titanium substrates exhibiting continuous micro and nano scale arrays, with increasing feature heights over the length of the array are reported. The resultant feature heights spanned 0–2 μm. Patterned gradient arrays of circular features with diameters of: 500 nm, 1 μm and 2 μm, spaced by twice the diameter were manufactured by the process using specially prepared titanium substrates. Patterns were exposed by electron beam lithography and the length of the patterned arrays was 15 mm or 20 mm. This work presents two selectivity amplification processes to achieve a gradient of feature heights ranging over the titanium array after consecutive reactive ion etching processes. The first, route A: a HSQ on Ti, gradient amplification process. The second, route B, a SiO_2 layer amplification transfer into Ti. The crucial initial gradient component deposited for the amplification process for both routes was a diffusion limited plasma polymerised hexane gradient. Etching using respective reactive ion etch chemistries for each gradient transfer through the various selectivity amplification layers (employing consecutive etch steps, in this way) enables a dual amplification for each route to manufacture. The original gradient is transferred into titanium as a function of the sum of the respective selectivities between the materials, using the appropriate dry etch plasma conditions. The substrates henceforth are referred to as inlays, and were tested for use as a high throughput platform for polymer replication by injection moulding. It is envisaged that the fabrication methodology and resultant topographies have use in a range of engineering applications. The overall selectivity to Ti for polymerised hexane is increased by more than 20 times using each dual amplification process.

© 2016 Published by Elsevier B.V.

1. Introduction

Bio-orientated gradient topographies are presented here. This research motivation proceeds from work which in the past has employed gels, discrete pillar topographies and limited height range pillar gradient topographies to establish that cells are influenced in many ways via a mechanism called mechanotransduction [1–4]. As the name suggests, this mechanotransductive property cells exhibit, refers to the process by which a cell transduces a force into a biological response [3,4]. Implicitly, it has been shown that the associated tension of a cell's cytoskeleton can be influenced by the stiffness of a culture substrate. The resultant forces of interaction on or by the cell, in turn affects the mechanotransductive processes. This was elucidated by varying the stiffness's of the culture matrices, which can influence the cell's phenotype, proteomic expression, biochemical signalling activity and overall homeostasis [2,4–6]. The understanding of this synergistic cell-substrate mechanism is, however, in its infancy [1,6].

Feature gradient substrates for polymer injection moulding or "inlays" and their polymer replicates which can be later used as moulds to cast elastomeric polymers from, have been manufactured. This is specifically to provide for a prospective cell culture substrate with an associated pillar stiffness spectrum spanning the known range of cellular influence [3,5,7]. Diffusion limited plasma polymerised hexane gradients (ppHex) have been crucially utilised to provide part of this novel gradient amplification manufacture process [8,9]. Titanium (grade II) was used as the bulk material into which the gradient amplification was made, via one the two individual selectivity amplification mediums trialled. The amplification was enabled via ppHex gradient profile transfer through the sacrificial layer by reactive ion etching (RIE). Although traditionally considered difficult, titanium tooling was used as the bulk material for fabrication of this high aspect ratio (HAR) inlay for polymer injection moulding [9,10]. Better inlay fill and a slower rate of polymer cooling within or around the features of a titanium inlay versus some other tooling solutions is exhibited [9]. The thermal performance of titanium also negates the need for variothermal heat retardation techniques to achieve amiable replication. Such complicated and expensive techniques involve plumbing or electrical heating at the inlay tool interface of the injection moulder to control and improve inlay fill,

* Corresponding authors.
E-mail addresses: a.connell.1@research.gla.ac.uk (A. Connell),
nikolaj.gadegaard@glasgow.ac.uk (N. Gadegaard).

polymer freezing and help optimise cycle time [9]. Other additions to the inlay fabrication process like surface modification by silanization or plasma treatment techniques are not necessary using this titanium fabrication methodology. Titanium also exhibits better corrosion resistance and stress tolerance than most of all other materials commonly used for polymer injection moulding tooling today.

2. Materials and methods

2.1. Titanium polishing

Water jet cut titanium pieces of 25 mm × 25 mm × 1 mm with an unprocessed surface roughness of approximately 3.5 μm Ra were polished by hand polishing and chemical mechanical polishing (CMP). Hand polishing was initially performed by sanding the titanium surface with sandpaper consecutively using 200, 450, and then 600 grade grit. Following this, felt brushes and a hand drill were used to polish the Ti surface using diamond polishing paste of 2 μm and 1 μm particle size. Next, an automated chemical mechanical polishing machine (Orbis, CMP) was used with nanometre scale SiO_2 grit (slurry, ~30 nm) to achieve a mirror finish. After polishing, the titanium substrates were sonicated in MF-319 microposit developer for 5 min. This assists removal of the contaminants from the hand polishing stage and also silica embedded in the surface within the grain boundaries of the Ti after CMP processing. Samples were subsequently cleaned by sonication in acetone, methanol, and IPA respectively for 5 min each. Averaged AFM microscopy shows a polishing capability of 3.0 nm ($\pm$1 nm) Ra. The average deviation in surface roughness was calculated by measurements taken over 3 samples, with 6 measurements each of scan size 12 × 4 μm on each sample scan (NanoScope software).

2.2. Sample preparation

Samples for route A, (Fig. 1A) were prepared for electron beam exposure by spinning a pipetted volume of 250 μl HSQ (Hydrogen silsesquioxane, Dow Corning) onto the titanium substrate at 6000 rpm for 60 s. This yielded an approximate layer thickness of 310 nm. The substrates were baked for 2.5 min at 90 °C on a hotplate. Post electron beam exposure, HSQ substrates were developed at ambient temperature (20 °C), using CD-26 for 30 s. An IPA wash bottle rinse and subsequent DI water rinse (for 2 & 5 min respectively) post development was found to reduce micro masking effects after the subsequent etching. For substrates which utilised a SiO_2 layer i.e. route B, (Fig. 1B), the deposition was performed by plasma enhanced chemical vapour deposition (PEVCD 80 Plus, Oxford Instruments). For route B, 8% conc. 2010 PMMA (Elvacite 2010, Lucite International) was spun onto a substrate at 4000 rpm for 60 s. Then a bilayer was spun by spinning a second resist layer atop the primary PMMA layer using 4% conc. 2041 PMMA for 60 s, at 5000 rpm (Elvacite 2041, Lucite International). The overall thickness was ~410 nm. This bi-layer later serves to provide masking for the deposition of a patterned nichrome (NiCr) metal lift-off layer (65 nm, Plassys MEB 550S, electron beam evaporator), after exposure and development of the resist (see Fig. 1B). After spinning, the substrate was oven baked at 120 °C for 15 min then transferred to a 180 °C oven for 8 h. A conductance layer of 30 nm aluminium was then evaporated onto the substrate.

2.3. Electron beam lithography

The thermal field emission gun was 100 keV (as standard for Vistec, VB-6), a 32 nA beam current was selected. The beam step size chosen was 19 nm and was used for the exposure of both resists for this
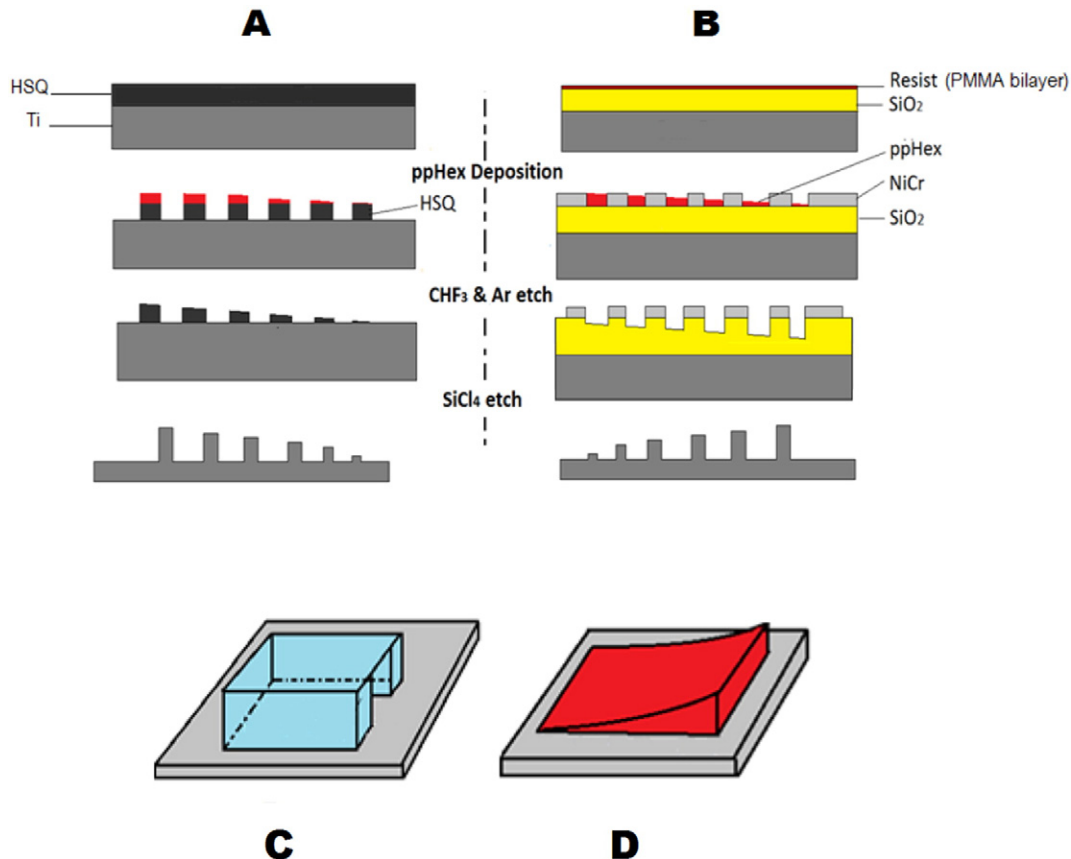

Fig. 1. (A) and (B) depict two routes to manufacture for the fabrication of pillar gradient arrays, made of titanium. (C) A diffusion limiting mask of dimensions: 20 × 15 × 8 mm, (D) a schematic of a ppHex gradient profile (mask removed) on a piece of titanium post deposition. Figure is not to scale.

work. For route A, i.e. HSQ substrates, CD-26 was used to develop the HSQ by immersion for 30 s, at 20 °C as stated prior. Dose testing showed that for $d = 500$ nm features exposure was best with 300 $\mu C/cm^{-2}$, 1 μm features required 510 $\mu C/cm^{-2}$ and 2 μm features were cross-linked using 650 $\mu C/cm^{-2}$. The exposure testing for route B is reported as optimal to clear the PMMA bilayer spun on 300 nm SiO_2 atop polished and clean 1 mm thick grade II bulk titanium. For $d = 500$ nm features 215$\mu C/cm^{-2}$, $d = 1$ μm features 230 $\mu C/cm^{-2}$ and $d = 2$ μm 240 $\mu C/cm^{-2}$ was optimal. The geometric arrangement (i.e. 2× diameter spacing) of the features at this mesoregion of size is causal to an inter-proximity effect. This is evident by the resulting dose trend required to clear features over the size range. This is also due to the nature of the generic Ti substrate configurations used for both route A and B. For route B substrates, the conductance layer was removed by immersing the substrate in the aluminium etchant CD-26 for 2.5 min prior to development. Development was then performed at 23 °C, in 1:1 MIBK: IPA for 60 s (MIBK, Methyl isobutyl ketone). The optimal development conditions and exposure relationship was determined by SEM analysis. Graduated markings exposed by electron beam lithography were patterned alongside the circular feature arrays to help locate and identify specific regions of the pillar gradient topography for characterisation purposes after fabrication.

2.4. Plasma polymerised hexane gradient

The patterned substrates were cleaned by an organic solvent cleaning process prior to deposition of ppHex. Then substrates were descummed in an O_2 (GaLa, PlasmaPrep5) barrel asher at 40 W for 40 s. This was found to significantly improve the adhesion and uniformity of ppHex gradients deposited. Depositions were performed in a custom built borosilate plasma deposition chamber. In the chamber, substrates were placed under a diffusion limiting (POP) Polyolefin plastomer mask. As the name suggests, the confined region of space under the diffusion limiting POP mask locally limits the gaseous flow through the plasma deposition chamber in the region under the mask. This augmented flow provides for a locally varied concentration of hexane species available to the polymerisation process. Polymerisation takes place on the surface of the patterned bulk Ti under the mask. The deposition profile on the substrate decays with distance from the opening toward the rear of the mask. The parameters impacting the ppHex gradient deposited include: the diffusion limiting mask dimensions, vacuum pressure, monomer flow rate, plasma power, the relative positioning of the sample within the chamber (fixed for this experimentation) and deposition time. Experimentally, the positioning of the diffusion limiting POP mask relative to the substrate patterning is also crucial. Gradients of ppHex deposited in this way are both controllable

and repeatable. An optimised process was found by experimentation that varied the prior stated parameters. This process can successfully be utilised to deposit a range of gradients of tuneable profile thickness up to ~200 nm at the thickest point decaying to 0 nm over 25 mm in length. Additionally, a spatial diffusion limiting mask of different dimensions would have the effect of augmenting the deposition profile [8].

Typically, the masked patterned Ti substrates were placed in the deposition chamber at a vacuum pressure of 5.1^{-1} mbar. Then hexane monomer was bled into the chamber by opening a control valve. After allowing the pressure to stabilise within the plasma chamber, environmental conditions were established as constant and the plasma was struck. The impedance matching component of the equipment was used to establish 100 W forward power with minimal reflected power. The plasma deposition was maintained for the required time for a given profile of ppHex (see Fig. 2). A linear deposition rate of ppHex was measured concurrently by quartz crystal microbalance output (QCM) and confirmed by AFM. The deposition rate was typically 0.0375 nm/s. The RF power was supplied in continuous wave mode (see also Fig. 1 C & D, Fig. 2) [8].

2.4.1. Gradient amplification (RIE)

After prior preparation the deposited plasma polymerised gradient masks over the patterned substrates for route A and B were etched using CHF_3/Ar RIE conditions (see Fig. 1). The RIE conditions were of gaseous ratio 25:18 sscm respectively. The RIE forward power was 200 W, chamber pressure was 30 mTorr, and the temperature maintained at 22 °C. (Plasmalab BP80, Oxford Instruments). This etch process was proven successful for transferring the reverse ppHex gradient profile into a SiO_2 layer, and HSQ patterned features in accordance with the selectivity ratio of the materials (see Fig. 2). The selectivity relationship was established by prior experimentation, and was found to be (SiO_2:ppHex) 3.9:1. The etch selectivity of HSQ was measured to be very similar at (HSQ:ppHex) 3.8:1. Fig. 2 was collated with averaged results from AFM measurements over 3 substrates, i.e. triplicate data sets. It elucidates ppHex deposition thicknesses (left) and resultant post etched SiO_2 gradient topographies (right). This gradient transfer was proven a highly repeatable process. The overall error statistically was ~2%. For ppHex-HSQ gradient profiles, the transfers were shown to be very similar to that of Fig. 2 for the same ppHex deposition and etch parameters.

Subsequently, to the initial gradient transfer from ppHex to a sacrificial selectivity amplification medium as elucidated. The common second RIE stage of the gradient transfer process for both routes A and B to manufacture was performed. This was executed using $SiCl_4$ RIE (S100, Oxford Instruments) to amplify the previously defined gradient profile of HSQ or SiO_2 respectively into the bulk titanium substrate.
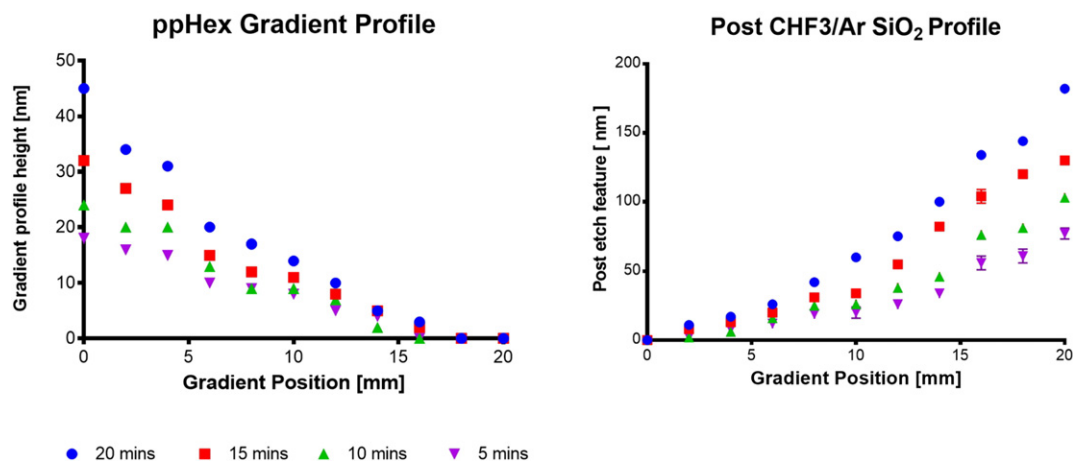

Fig. 2. The deposited ppHex gradient profiles (left), and their etched SiO_2 profile correlations (right). The ppHex gradient masks were etched to ablation using CHF_3/Ar RIE, monitored by interferometry.

The plasma parameters selected were gaseous flow rate 18 sscm, 200 W forward power and chamber pressure 9 mTorr which was maintained at 20 °C. Monitored interferometry was used to determine the end of the etch. The selectivity between HSQ and SiO_2 to Ti in these conditions is reported to be 1:13.3 for the parameters used.

2.5. HSQ gradient amplification

The exposed area of the negative resist by electron beam lithography, defines the pillars cross-sectional profiles after development and the respective etch steps (see also Section 2.3). This can be successfully varied from the circular experimental standard reported. In order that a gradient profile can be made of the post development, uniform height HSQ pillars a ppHex gradient was deposited atop the HSQ patterned array on the substrate and subsequently measured by AFM. The deposited ppHex gradient was in accordance with the slope of the topography for a 20 min deposition profile (Fig. 1A, see also Fig. 2 left). The ppHex gradient mask deposited atop (and amongst) the HSQ pillars was etched by monitored interferometry to total ablation of the gradient film. This creates an amplified reverse gradient profile in the HSQ pillars using CHF_3/Ar RIE (Plasmalab, BP 80 Oxford Instruments). The ppHex gradient transfer of a profile 45 nm decaying to 0 nm, (see Fig. 2, left, 20 min) into the sacrificial amplification medium (i.e. HSQ pillars) for this route to manufacture took 5.6 min using CHF_3/Ar RIE conditions as described. The plasma conditions were intrinsically selected to offer almost negligible ablation of Ti. The gradient of HSQ pillars made by this process, then served to mask the Ti variably over the array length for the next etch step. Subsequently, $SiCl_4$ RIE (S100, Oxford Instruments) to finish the gradient substrate manufacture was performed (Section 3.1, see Fig. 3). For the initial gradient transfer prior

experimentation had shown that for ppHex in CHF_3/Ar RIE plasma the etch rate is ~9.1 nm/min for ppHex. The etch rate of HSQ was found to be ~38 nm/min under the same conditions. $SiCl_4$ RIE for 93.5 min was performed to transfer and amplify the HSQ gradient array into the bulk Ti substrate. The interferometer laser was focused at a prior calculated point along the gradient to detect maximum etch amplification efficiency (see Section 4.1). This process resulted in a titanium gradient array ranging in height from 0–~2.0 μm. The achievable feature height was found to depend on the aspect ratio of the particular array geometry. It was recorded that the etch rate of Ti in $SiCl_4$ RIE is 22 nm/min, and HSQ ~1.5 nm/min. The original 20 × 4 mm patterned array substrates and their polymer injection moulded replicas are represented in Fig. 3.

2.6. SiO_2 gradient amplification

300 nm (PEVCD) SiO_2 was deposited atop a polished and clean Ti substrate. The SiO_2 thickness was chosen in consideration of a ppHex gradient 45 nm at its thickest point i.e. a 20 min deposition profile being etched to total ablation (see Fig. 2). The hard mask which defined the cross-sectional shape of pillar's by the SiO_2 masking system was a pre-patterned NiCr hard mask atop the deposited SiO_2. CHF_3/Ar RIE was used to etch the ppHex gradient (see Fig. 1B). The hard mask utilised to define the pillars cross-sectional shape for this route to manufacture, can also be varied successfully from the experimental standard. The SiO_2 thickness required was calculated with respect to both the initial profile transfer from ppHex-SiO_2, and with consideration of the depletion of the SiO_2 hard mask gradient in the subsequent $SiCl_4$ etch process over titanium. Governing the limitations of fabrication were: the selectivity of the respective materials; the profile or slope of the gradient; and the anisotropic limitations of deep etch Ti processes
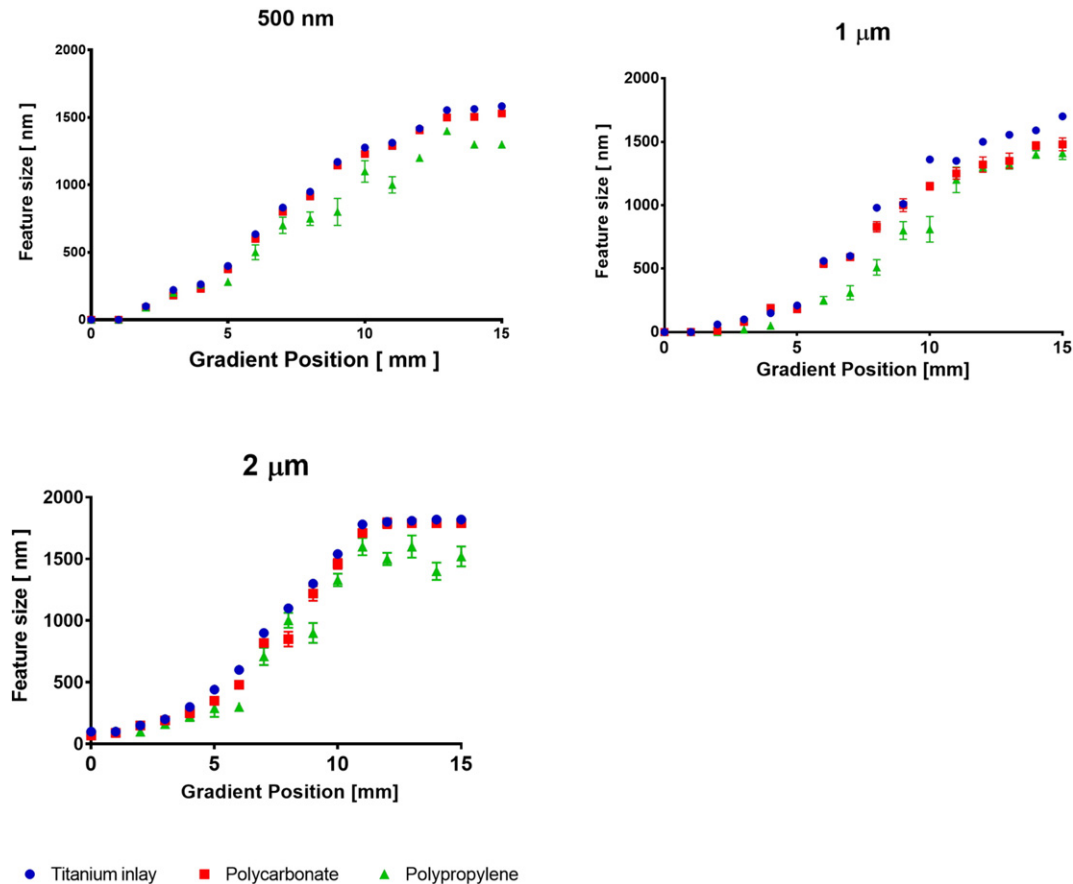

Fig. 3. The AFM measurement data above represents the Ti inlays manufactured by the HSQ amplification process i.e. pillar height. Also shown is the profilometry data for polymer replicates (PC and PP), manufactured by injection moulding. The measurements are inverse for the polymer replicates.

using RIE. The significance of the original gradient, its transfer into the respective substrata, and its contribution to the efficiency of the overall gradient manufacture are discussed later (see Section 4.1).

Experimentally, the substrate was prepared as previously specified for ppHex gradient deposition. The diffusion limiting mask was placed over the pattern strategically and the duration of the deposition was 20 min (see Fig. 2, left). The substrate was then etched in CHF_3/Ar RIE plasma conditions for 6.1 mins (see Section 2.4.1). This completed the initial ppHex gradient transfer etch to the sacrificial amplification medium i.e. SiO_2 for this, route B. The substrate was then etched in $SiCl_4$ RIE for 103 min. SEM images of the topographies are shown in Fig. 4. The image set comprises 2 separate substrates with individual feature arrays patterned originally to 15 mm × 2 mm. For 2 μm and 1 μm diameter features the arrays were patterned on the same substrate (Fig. 4, A–F), and the etch times were as stated above. RIE lag due to the varying aspect ratio exhibited at this size range of feature diameter limited the gradient height range span achievable for d = 500 nm features, in comparison to that of d = 1 μm and 2 μm features. Thus, an identical protocol was followed for the d = 500 nm array substrate fabrication (Fig. 4, G–I). However, the etch times required were found to be necessarily slightly longer, taking 6.5 min to etch ppHex-SiO_2 using CHF_3/Ar RIE and subsequently 121.5 min $SiCl_4$ RIE etch time. The complete analytical data set for both inlays manufactured by route B and their replicates are shown in Fig. 5.

2.7. Polymer injection moulding

The manufactured Ti substrates were used as inlays for polymer injection moulding. Injection moulding uses polymer beads, incrementally heated within a screw thread to their appropriate liquid state. In this case the temperature was for polypropylene (PP) 250 °C and polycarbonate (PC) 280 °C. The polymer injection moulder (Victory 28, Engel GmbH) after heating the polymer then injects it through a nozzle into a tool cavity which contains the patterned Ti inlay. This enabled the manufacture of a "negative polymer substrate" as per the flow of polymer into the defined tooling space which is subject to certain controllable conditions. The moulding parameters to an extent define the finished part's characteristics. This type of polymer injection moulding using the manufactured titanium inlays offers throughput cycle times of down to below 15 s. For these inlays the best samples were moulded with cycle times for PP of 16 s and PC, 20 s. A low cycle time enables high throughput manufacture of polymer replicas more efficiently. The appreciable repeatability and thermal performance owing to the use of a Ti inlay for the moulding of these unique polymer topologies is a major advantage (see Section 1.0). [9] The parameters used for the replication of the inlay substrates described in this study were as follows: mould injection pressure: 1000 bar, shot volume 4 cm^{-3}, cooling time ~ 7 s. The tool temperature which is the piece of the equipment within which the inlay is placed for the inlay replication was for PC 80 °C and for PP 50 °C.

3. Results

For both routes A and B (see Fig. 2) the ppHex deposition, and consecutive dual etch protocol as previously described was critical to the successful manufacture of gradient pillar topographies using the individual selectivity amplification techniques into bulk Ti. The transfer and amplification of ppHex gradients into patterned HSQ, and its
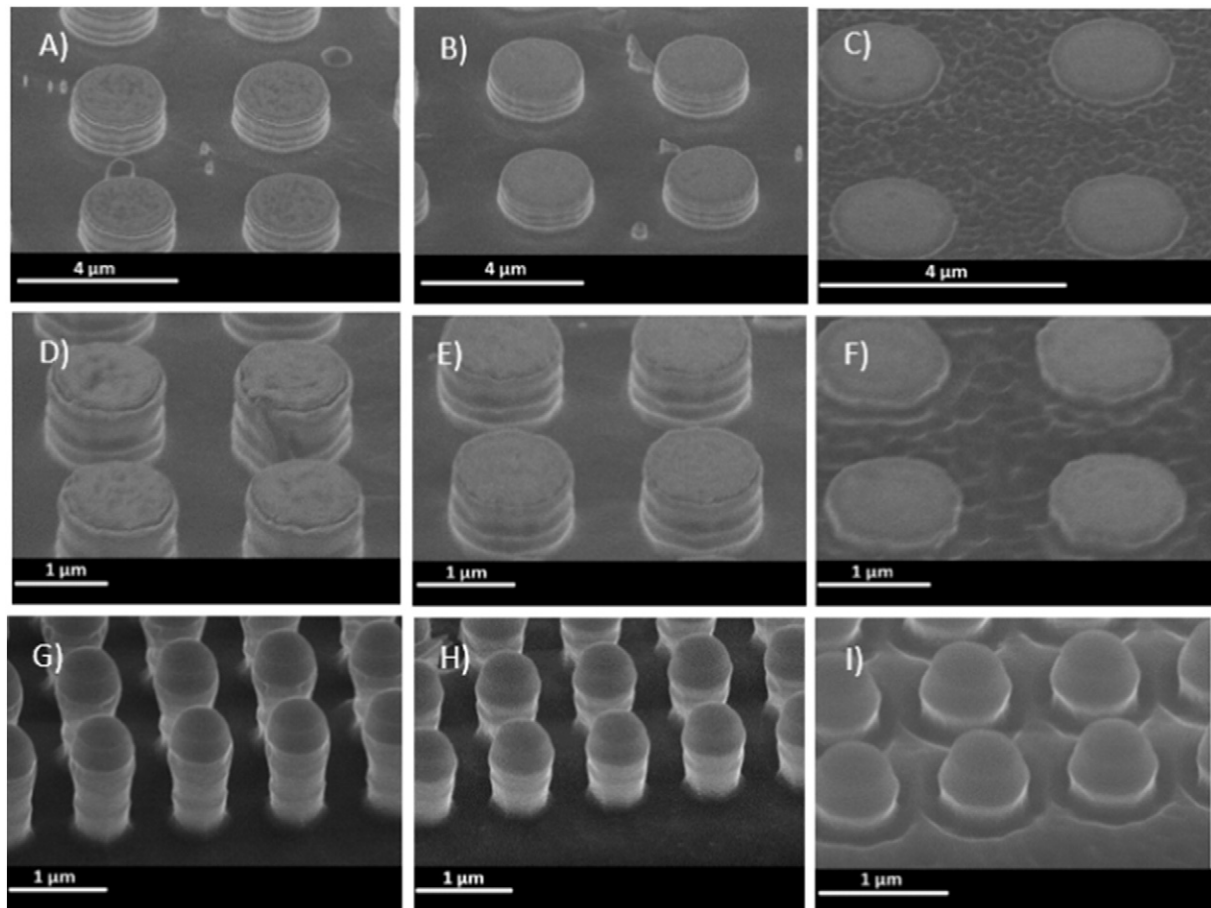

Fig. 4. Pillar topographies manufactured by SiO_2 amplification (route B). (A–C, D–F) represent one sample featuring d = 2 μm and 1 μm arrays respectively. G–I represents a separate sample, d = 500 nm. Images in the left hand column were taken at (gradient position) X = 8 mm, middle X = 4 mm, right X = 0.2 mm.

500 nm

1 μm

2 μm

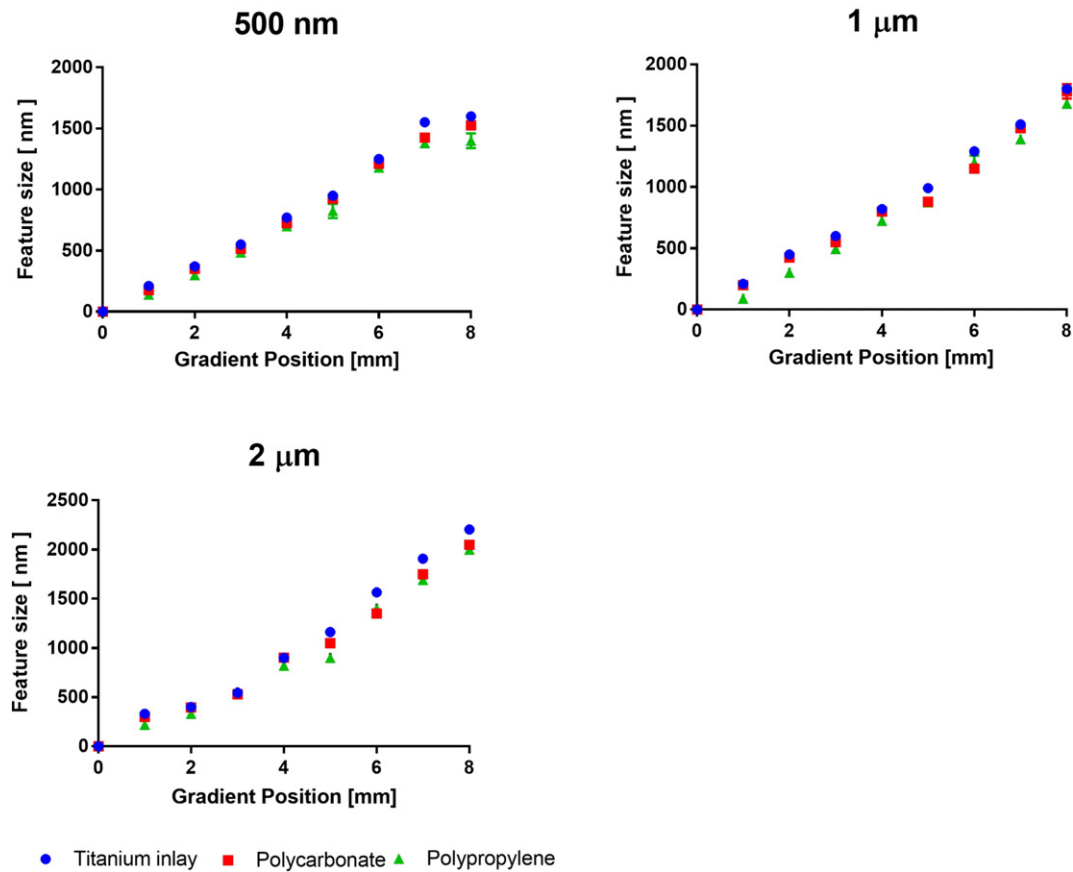● Titanium inlay   ■ Polycarbonate   ▲ Polypropylene

Fig. 5. The AFM measurement data above represents the Ti inlays manufactured by route B, i.e. pillar height. Also shown is the inverse profilometry data for polymer replicates (PC and PP), manufactured by injection moulding. RIE transfer dynamics explain the shortened gradient span from the original patterned array length.

subsequent use as a sacrificial amplification layer, offers appreciable profile transfer amplification capabilities into bulk Ti. However, the route B methodology of the 2 trialled during the course of this experimental investigation was most successful.

3.1. Titanium pillar arrays and replicates, for manufacture route A

Both in terms of the overall success of substrate fabrication and inherently for its use in polymer injection moulding. HSQ (route A) performed with diminished functionality overall, by comparison to the SiO_2 (route B) amplification technique investigated. Some micro masking was observed after development of samples manufactured by route A. The consecutive gradient transfer etches into Ti pillars as described in the methodology amplified these defects. This was reduced to an extent by thoroughly cleaning the substrates with IPA and deionised water immediately post development. Solvent cleaning significantly reduced micromasking. The consecutive dual etch amplification process increased the overall selectivity achievable using the sacrificial HSQ amplification strategy for gradient manufacture, by route A, by in excess of 20 times. That is, with respect to the achievable selectivity ratio attainable by direct etching of ppHex over titanium which offers a selectivity ratio of 1:1.5 (ppHex:Ti) in $SiCl_4$ RIE conditions. It is also worth noting that ppHex films show limited mask integrity over long etches in $SiCl_4$.

3.2. Titanium pillar arrays and replicates, for manufacture route B

Both routes A and B to manufacture are applicable for successful gradient fabrication, and exhibit similar resultant cumulative selectivities. However, the manufacture methodology shown for route B and further elucidated herewith has some distinct advantages over the HSQ

method, route A. The advantages, include more preferable feature sidewall angles, improved repeatability and better finished inlay surface pros in general are exhibited. For route B, the areas void of features had significantly lower surface roughness averages (12 nm ($\pm$2 nm)) than those measured for route A (19 nm ($\pm$5 nm)).

4. Conclusions and discussion

The manufacture routes presented for making patterned feature gradient topographies of bulk Ti, and their subsequent polymer replication has proven successful. Originally the ppHex gradient transfer into the amplification medium, for route A and B has a deterministic role in the subsequent etch capability of the finished Ti feature gradient substrate. Anisotropic sharpening of finished Ti features was observed to result from etch durations in considerable excess of those stated for $SiCl_4$ RIE. This non-amiable trait of long duration RIE could be improved for this process by etching using inductively coupled plasma (ICP) etch conditions. ICP processing in place of the $SiCl_4$ RIE step would result in a greater gradient feature height span being achievable due to the preferable selectivity. Selectivity values are reported to be as high as 1:40 for SiO_2:Ti, using ICP etching. [11].

4.1. Limitation of manufacture

The overall efficiency of the gradient transfer process described for both routes by this work is a dynamic function. The sum of the bulk selectivity of the amplification materials during respective, cumulative etches toward manufacture can effectively be considered a constant. The function has dynamic limits set by the slope of the profile of the masking gradient with respect to the co-ordinate position along the length of the array of the masking pillar tops for HSQ on titanium, i.e.

route A. Alternatively, but similarly, this dynamic limitation is also deterministic for the overall amplification transfer of a gradient of ppHex via SiO_2 to Ti. However, a slightly more intricate relationship exists when pillar gradients are amplified in this way. Generally the finished profile can geometrically be described as an amplified translation of the ppHex gradient originally deposited for both routes A and B, but transferred into Ti. The overall selectivity to Ti for route B is bound both by the original thickness of the SiO_2 strata but dissimilarly to route A, also bound by the slope profile at the base of the features along the length of the gradient. During $SiCl_4$ RIE the dynamic effective selectivity of the respective gradient mask was critically considered. For both routes the masking system efficiency is differentially dependent on the variables stated. However, concisely put for route A, the limiting parameters are the slope profile of the HSQ pillar tops, their max. to min. Height deviation, and the material selectivity ratio. For route B gradient transfer, we consider the slope along the base of pillars over the length of the array as a dynamic component of the function of transfer efficiency. This is bound with respect to the deviation of max. to min. SiO_2 pillar height, the originally deposited SiO_2 strata thickness, and the material selectivity ratio. By graphing each system for route A and B prior to the $SiCl_4$ etch stage it was possible to determine the location along the gradient at which upon total ablation indicates maximum efficiency of the gradient amplification for both routes. This location was selected and used for monitored interferometry during RIE. This aided prevention of over and under etching by enabling focused laser interferometry positioning without which adversely reduced feature height spans can result.

Acknowledgements

References

[1] P.M. Reynolds, R.H. Pedersen, J. Stormonth-Darling, M.J. Dalby, M.O. Riehle, N. Gadegaard, Label-free segmentation of Co-cultured cells on a nanotopographical gradient, Nano Lett. 13 (2) (2013) 570–576.

[2] V. Damljanović, B.C. Lagerholm, K. Jacobson, Bulk and micropatterned conjugation of extracellular matrix proteins to characterized polyacrylamide substrates for cell mechanotransduction assays, Biotechniques 39 (6) (2005) 847–851.

[3] S. Ghassemia, G. Meaccib, S. Liua, A.A. Gondarenkoa, A. Mathura, P. Roca-Cusachsc, M.P. Sheetz, J. Hone, Cells test substrate rigidity by local contractions on submicrometer pillars, Proc. Natl. Acad. Sci. U. S. A. 109 (14) (2012) 5328–5333.

[4] J. Eyckmans, T. Boudou, X. Yu, C. Chen, A hitchhiker's guide to mechanobiology, Dev. Cell 21 (2011) 35–47.

[5] A.J. Engler, S. Shamir, H. Lee Sweeney, D.E. Disc, Matrix elasticity directs stem cell lineage specification, Cell 126 (2006) 677–689.

[6] S.-Y. Tee, F. Jianping, C.S. Chen, P.A. Janmey, Cell shape and substrate rigidity both regulate cell stiffness, Biophys. J. 100 (5) (2011) 25–27.

[7] D.E. Discher, P. Janmey, Y.-l. Wang, Tissue Cells Feel and Respond to the Stiffness of Their Substrate, 310 (5751), 2005 1139–1143.

[8] R.H. Pedersen, D.J. Scurr, P. Roach, M.R. Alexander, N. Gadegaard, Full-thickness characterization of plasma polymerized hexane films irradiated by an electron beam, Plasma Process. Polym. 9 (1) (2012) 22–27.

[9] R.H. Pedersen, Q. Xu, J.M. Stormonth-Darling, N. Gadegaard, Strategies for high quality injection moulding of polymer nanopillars, Macromol. Mater. Eng. 300 (2) (2015) 172–180.

[10] F. Fracassi, R. d'Agostino, Chemistry of titanium dry etching in fluorinated and chlorinated gases, Pure Appl. Chem. 64 (5) (1992) 703–707.

[11] E.R. Parker, B.J. Thibeault, M.F. Aimi, M.P. Rao, N.C. MacDonald, Inductively coupled plasma etching of bulk titanium for MEMS applications, J. Electrochem. Soc. 152 (10) (2005) 675–683.